UNIVERSITY OF BATH

Citation for published version:
Evans, S & Keogh, P 2016, 'Efficiency and running temperature of a polymer-steel spur gear pair from slip/roll ratio fundamentals', *Tribology International*, vol. 97, pp. 379-389. https://doi.org/10.1016/j.triboint.2016.01.052

DOI:
10.1016/j.triboint.2016.01.052

Publication date:
2016

Document Version
Peer reviewed version

Link to publication

Publisher Rights
CC BY-NC-ND

University of Bath

Alternative formats
If you require this document in an alternative format, please contact:
openaccess@bath.ac.uk

General rights
Copyright and moral rights for the publications made accessible in the public portal are retained by the authors and/or other copyright owners and it is a condition of accessing publications that users recognise and abide by the legal requirements associated with these rights.

Take down policy
If you believe that this document breaches copyright please contact us providing details, and we will remove access to the work immediately and investigate your claim.

Download date: 05. May. 2023

Efficiency and running temperature of a polymer-steel spur gear pair from slip/roll ratio fundamentals

S.M. Evans[a,b] (s.m.evans@bath.ac.uk), P.S. Keogh[a]

[a] Department of Mechanical Engineering, University of Bath, Bath, BA2 7AY, UK

[b] Rotork plc, Brassmill Lane, Bath, BA1 3JQ, UK

ABSTRACT

A new methodology to predict the transient operational temperature of a polymer-steel gear pair under loaded running is presented. For the involute gear form, rolling and sliding leads to a loss of gear efficiency and generation of heat in the contact zone. The power dissipated is used to set the conditions for a series of rod on disc experiments. The rod-on-disc data are processed in a time averaging procedure, which allows prediction of the complete gear temperature. This is assessed with analytical and finite element models to validate the predicted temperature rise against the experimental data. The significance is that the experimental procedures may be used to assess gear thermal performance without testing full gear pairs.

Keywords: gear efficiency; polymer gear temperature; slip/roll ratio; temperature prediction

1. Introduction

Spur gears that are machined or injection moulded from polymers are becoming increasingly prevalent in geared systems since they can be manufactured cost effectively, especially when moulded. They also have a lower inertia than metallic gears, which can be advantageous in terms of the dynamic response of a gear train used in low power transmission applications. In addition, as the number of polymer gears manufactured per year rivals that of metallic gears there is a desire to utilise them in higher power applications. Metallic spur gears have been well-researched and developed and it is now possible to design them with a high degree of confidence, taking account of strength and wear. However, it is less straightforward to calculate the strength of polymer spur gears due to the nonlinear properties of polymers and the limited work that has been done to investigate their wear mechanisms. This paper investigates the contact mechanism between two straight cut spur gear teeth (one metal and one polymer) and how it results in heat generated in the zone of contact.

The contact in a straight cut involute spur gear pair has both rolling and sliding elements as first documented by Breeds *et al*. [1]. Pure rolling occurs at the point at which the contact is in line with the centres of both the pinion and the gear, however, this occurs only at an instantaneous point. As the contact approaches this point and then moves away from it the sliding velocity decreases and then increases, respectively. This action can be modelled using the concept of equivalent cylinders, as reported by Hamrock *et al*. [2] who associates, for each point in the contact sweep, two cylinders of differing radii in contact with relative velocities determined by the rotation of pinion and gear. The sliding velocity can then be calculated through the contact sweep, which will vary through the stroke. The geometry of a gear is such that fine details of the size and shape of the teeth are superimposed upon the overall diameter of the circular gear. A full thermal analysis of the complete gear geometry would therefore be complex and an alternative predictive model based on the equivalent cylinders analogue would be preferable. This alternative model would also require experimental validation, for example, from an axially aligned steel rod in sliding contact with a polymer disc. The manner in which experimental and predicted results are compared would be critical for the validation process and this provides a focus for the procedures described in this paper.

The works of Hooke *et al.* [3] and Breeds *et al.* [1] make substantial inroads into understanding how spur gears run together and what the contact mechanics are of the gear teeth. In particular, the actions of rolling and sliding between the driven and driving gear are described. Furthermore, they indicate how this geometry driven contact, so particular to involute spur gears, may influence the efficiency of any given gear pair as well as resistance to wear, which are both instrumental in temperature rise. With reference to polymer-steel contact in involute gears a study was conducted using a Bowden-Leben stick-slip machine, which is a conventional tribometer utilising a pin sliding against a flat surface (Bowers *et al.* [4]). For steel running against nylon, values of 0.37 and 0.34 for static and dynamic friction, respectively, were published. Clearly, the materials chosen for the gears

will have a large effect on the friction and associated efficiency, which were measured by Walton *et al.* [5]. The efficiency ranged between 88% and 98% depending on material, load and speed. Overall, the material is a driving factor in the increase or decrease of efficiency, but the geometry, hence slip ratio is also important. Xie and Williams [6] made progress in predicting the coefficient of friction and wear between a randomly rough hard surface and a softer surface. They used a technique developed by Greenwood and Williamson [7] and expanded it to include specific plastic micro cutting of the softer material by the harder. Although progress has been made in the link between this and the actual contact mechanism, much is still to be done to quantify it completely. Indeed, in medical prosthetics, there has been much experimentation to validate a particular geometry of ball and cup of defined materials. Fisher *et al.* [8] found that surface roughness contributes greatly to the wear of a polymer in contact with a metal. They also concluded that the wear was not dependent on sliding velocity, however, the maximum sliding speeds used were 240 mm/s, which are lower than those generally experienced by gear teeth.

Blok [9] describes the concept of flash temperature, which provides a method for estimating the likely temperature between two contacting and sliding surfaces. If the flash temperature for a polymer-steel spur gear pair is above the melting point of the polymeric material, failure of the component will clearly be imminent. This has been expanded and improved upon on by Samyn and Schoukens [10] and also by Conte *et al*. [11] with inclusion of thermal diffusivity for the material in question. A numerical solution has been developed specifically for the application to spur gear teeth by Mao [12], who accounts for the effects at the tooth tip as the mesh starts and finishes, but it is considerably more complex than the Blok model. Attempts to reduce the running temperature to see if that materially affects the wear rate of the gears were carried out by Kim [13] and Duzcukoglu [14] by drilling small holes through the base of the root of the tooth to let air circulate more freely across the tooth flank. These studies found that reducing the running temperature of the gears also reduces the wear rate. Other experiments include loaded running of gears for temperature measurement and wear measurement, as in the work of Hooke *et al.* [15].

Another test method uses a back-to-back apparatus with one electric motor driving through the gear pair under investigation to the driven motor, which acts as a generator and so provides the load. This was undertaken by Senthilvelan and Gnanamoorthy [16] and surface features were observed that are relevant. However, no further analysis or conclusions for wear mechanisms or temperature rise were given. Hooke *et al.* [15] used a four-square rig with a single electric motor to drive two sets of spur gears connected across two parallel shafts. The driven gears were manufactured from case hardened steel, whilst the others were test polymer gears, as reported by Mao *et al.* [17] and [18]. The load was applied to the system through a lever arm, even as the gears became worn. These studies were concerned with how temperature and differing materials affect the wear of the gears. Acetal was used as the gear test material and it was concluded that it has a critical limit in terms of slip/roll beyond which complete failure of the material occurs due to thermal effects.

Analytical models have been constructed that predict the temperature rise around a contact area such as in the work of Vick and Furey [19] who used a Green's function approach. For steel running against a polymer the temperature rise should not exceed the polymer softening or melting temperature as this would clearly result in a catastrophic failure. This is the basis for a concept of the pressure-velocity limit for a polymer as proposed by Archard [20]. In a study by Walton *et al*. [21], load sharing of polymer gears was investigated using computational finite element techniques. They were concerned only with the loading between the gear teeth. A thermoelastic model can be created using finite element techniques as done by Taburdagitan and Akkok [22]. It is of interest as it illustrates some of the difficulties associated with producing this type of model. The model mesh was refined around the gears and the driven gear was considered loaded via a torsional spring at its centre. The conclusion was that tip relief of the gear teeth is important to the temperature rise as applying it can help to reduce the slip speed when the driving gear initially touches the driven gear and load transfer occurs. In a study by Unal *et al.* [23] of extremely high pressures of steel rubbing against a polymer, it was found that the wear rate of a polymer in this case is not strongly dependent on the pressure applied.

In this paper, an experiment involving an axially aligned steel rod applied to the circumference of a polymer disc is described. This experiment was augmented to run a full gear pair, of which the running temperatures were also measured. An analytical thermal model is formulated to predict the temperature rise in the axially aligned rod on disc experiment. A finite element model was also employed as an alternative method for prediction, though limited to a fixed heat source on the disc. This simplification is used to reduce the complexity of a full gear model and the mesh density required at the contact. Lee *et al*. [24] present a case in which a high mesh density is implemented for asperity-asperity interaction. Finally, a novel method of time averaging is presented to directly correlate the aligned rod on disc experiment with full the gear pair experiment.

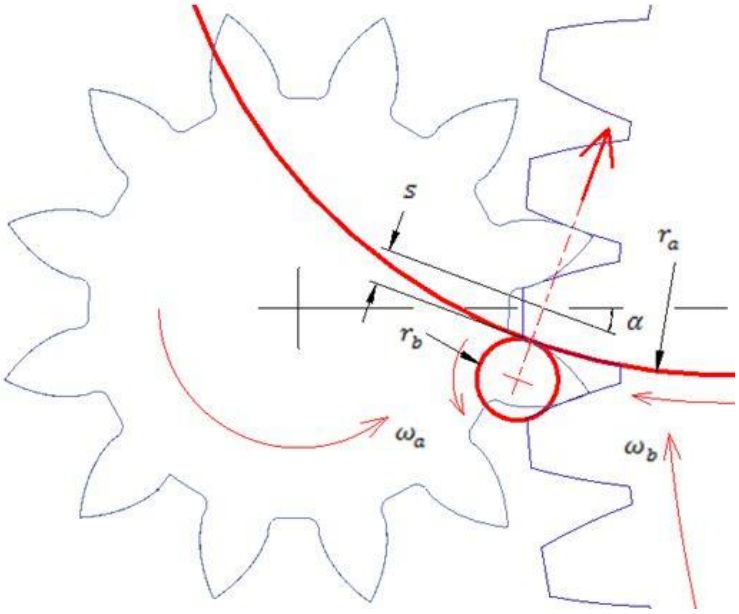

Fig. 1. Equivalent cylinders.

2. Geometry, flash temperature, loadings and heat flux evaluation

In this section, pertinent evaluations are made that are appropriate for geometric and material parameters associated with the experimental system and gears considered in Section 3.

2.1. Geometry

A feature of the involute profile that is known, but not generally considered significant, is that slip occurs between the teeth flanks. This results in a reduction in efficiency of around 1 – 2 % [5]. However, in an unlubricated polymer-steel gear pair it gives rise to heat generation. In the line diagram shown in Fig. 1, two contacting surfaces are represented by two separate cylinders of radii r_a and r_b. The rotational speeds of these cylinders are equal to those of the gears, respectively. This technique is described by Hamrock *et al*. [2] and the slip speed is

$$v = (r_{bg} sin\alpha + s)\omega_b - (r_{ag} sin\alpha - s)\omega_a \quad (1)$$

where r_{ag} is the pinion pitch radius, r_{bg} is the gear pitch radius, α is the pressure angle (rad), s is the distance of the point of contact from the centre line, ω_a is the rotational speed (rad/s) of the pinion, and ω_b is the rotational speed (rad/s) of the gear. Accordingly, $r_a = r_{ag} sin\alpha - s$ and $r_b = r_{bg} sin\alpha + s$.

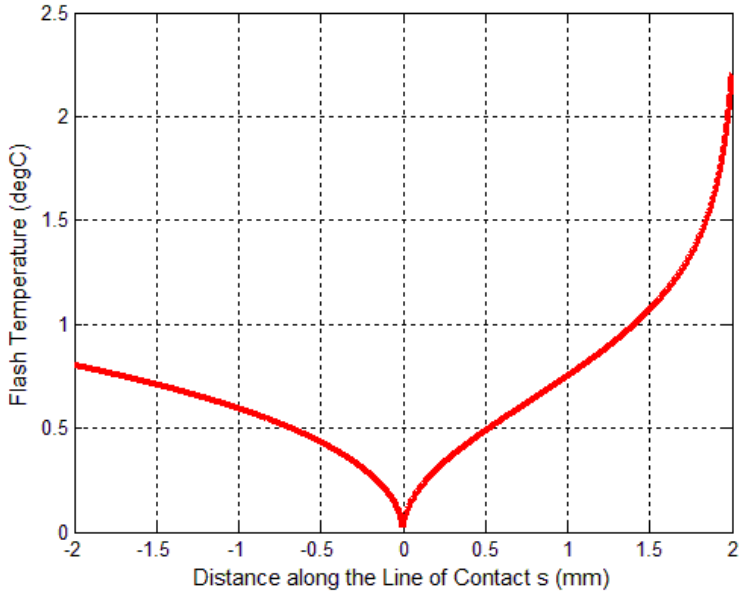

Fig. 2. Flash temperature profile. Data used: A = 1.1, k = 0.25 W/m/K, c = 500 J/kg/K (steel), c = 1670 J/kg/K (nylon), b, v and q_{av} vary through stroke according to geometry of contact.

2.2. Flash temperature

Blok [9] proposed that if two surfaces are rubbed together, heat will be generated at the interface giving rise to a flash temperature. Because of the transient and constrained nature of the contact, this temperature rise will be higher than expected for the load and speed conditions of a gear pair. The flash temperature is given by

$$T_f = A\frac{q_{av}}{\sqrt{kc}}\sqrt{\frac{b}{v}} \tag{2}$$

where v is the sliding velocity, b is the length of the heat source in the sliding direction, k is the thermal conductivity of the material, c is the specific heat per unit volume, A is a form factor offered by Blok, which is specific to the distribution of the heat flux, and q_{av} is the average heat flux input over the length b. Figure 2 shows a typical evaluation of T_f for a gear, where v has been evaluated from Eq. (1) for $-2 \le s \le 2$ (mm). However, T_f is only a transient parameter and takes no account of the gradual accumulation and cyclic nature of the heat generation in a continuously rotating power driven gear pair. Hence the flash temperature alone cannot provide the final operating temperature of the gears.

2.3. Loadings and heat flux evaluation

The force generated between the driving and driven gear acts normal to the two gear teeth curvatures at their instantaneous point of contact and can be calculated from the driving torque, the acting radius and the pressure angle of the involute. The force normal to that point of contact is given by

$$F_{cn} = \frac{\tau}{r_a} \cos \alpha \tag{3}$$

where τ is the input torque and r_a is the reference radius of the pinion (Fig. 1). In the case of the studied gear pair, $\tau = 0.85$ Nm and $r_a = 6$ mm, which yields a normal force of 133 N. The materials investigated are steel (EN 1.1186, EN8) for the pinion and a polymer (POM Delrin 100) for the gear. The dynamic coefficient of friction between these materials is taken as 0.34 from Bowers *et al.* [4]. Since polymer-steel gears are generally unlubricated, the losses arising from a potential increase in friction need to be assessed. It is important to analyse the resulting temperature increase in order to be able to ensure that the polymer is able to operate within its temperature limit. It follows that as the equivalent cylinders change to represent the contacting radii through the tooth stroke and the normal force remains constant, the penetration of the steel gear into the polymer gear changes. Hence the area onto which the heat input is applied also changes. To this end, the deflection must be calculated to determine the heat flux for any given point in the contact between the teeth.

Table 1

Contact stress at points along the line of contact s.

s (mm)	**0.0**	**0.1**	**0.2**	**0.3**	**0.4**	**0.6**	**0.9**	**1.1**	**1.4**
σ_{max}(MPa)	74.5	73.1	71.7	70.5	69.3	67.2	64.5	62.9	60.9
b (mm)	0.73	0.73	0.73	0.72	0.72	0.71	0.71	0.70	0.69
r_b(mm)	12.83	12.73	12.63	12.53	12.43	12.23	11.93	11.73	11.43
r_a(mm)	2.05	2.15	2.25	2.35	2.45	2.65	2.95	3.15	3.45
v (mm/s)	0	61	121	182	243	364	547	668	850

The maximum stress and circumferential length of contact area for a cylinder pressing against a cylinder is given by Hertzian contact stress theory [25]. Let subscript *a* denote the steel pinion material and subscript *b* the gear polymer material. Then

$$C_E = \frac{1 - v_a^2}{E_a} + \frac{1 - v_b^2}{E_b} \tag{4}$$

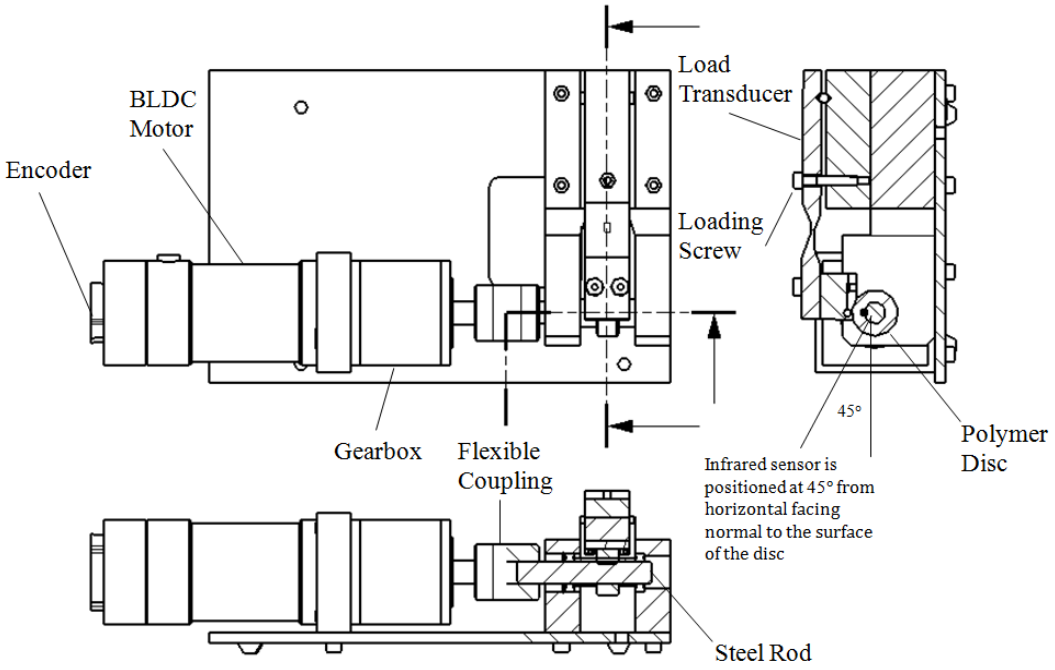

Fig. 3. Axially aligned steel rod-on-disc facility.

where E is the Young's modulus and υ is Poisson's ratio. The maximum Hertzian stress is

$$\sigma_{max} = 0.798\sqrt{\frac{F_{cn}(r_a+r_b)}{2C_E w r_a r_b}} \tag{5}$$

and the circumferential length of contact due to penetration is

$$b = 1.6\sqrt{\frac{2F_{cn}C_E r_a r_b}{w(r_a+r_b)}} \tag{6}$$

where w is the gear width and F_{cn} is the normal load. For completeness, the penetration depth is

$$\delta = \frac{2F_{cn}C_E}{\pi w}\left[\frac{2}{3} + \ln\frac{4r_a}{b} + \ln\frac{4r_b}{b}\right] \tag{7}$$

Given a disc width of 10 mm, Table 1 shows evaluated variation of parameters with variation of distance along the line of contact s as the teeth move through a contact cycle.

The instantaneous power dissipated into the polymer follows as

$$P_T = \phi F_{cn}\mu v \tag{8}$$

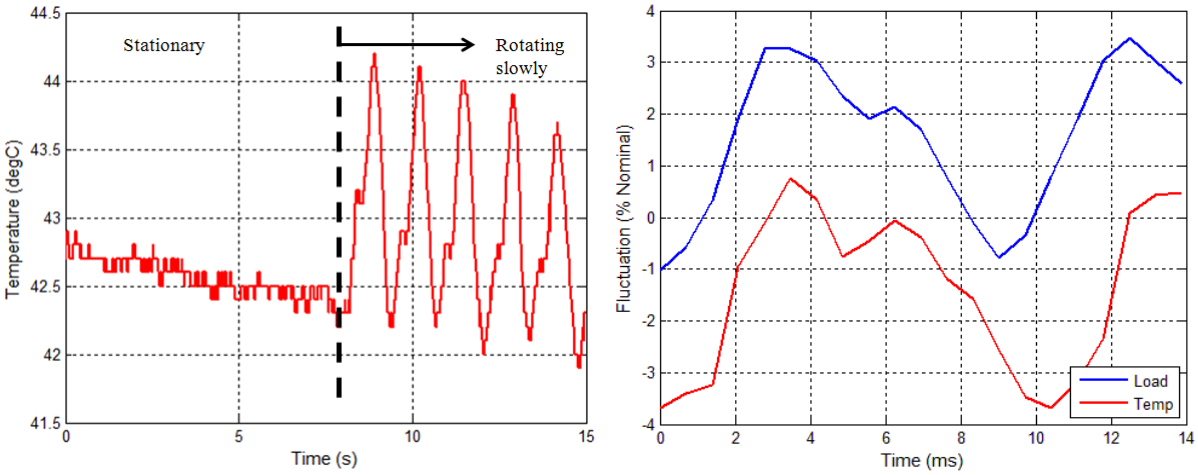

Fig. 4 (a) Slow rotation disc surface temperature; **(b)** Synchronisation of load and temperature.

where ϕ is a fractional coefficient and μ is the coefficient of friction (0.34). The precise value of ϕ will thermal conductivity values and the relative size of the disc compared to the rod. For the experimental system, $\phi \approx 1$ is a good approximation. The heat flux into the polymer is

$$Q_T = \frac{\phi F_{cn} \mu v}{wb} \tag{9}$$

Using the previous data, this is evaluated as 0.848 W/mm^2 for s = 0.2 mm. This is purely the heat generated between the two contacting surfaces. The relative proportions of that heat transport that are shared between the polymer and the steel are accounted for in the models presented in the later sections.

3. Experimental thermal assessment

The assessment of temperature rise was made in two separate experiments. The first was designed to emulate the equivalent cylinders (Fig. 1) and consisted of a disc rotating against a loaded, but stationary and axially aligned rod. The second experimental arrangement measured the temperature rise in a complete gear. The purpose of the axially aligned rod-on-disc experiments is to replicate the range of slip and torque conditions expected from a complete gear design. In Section 5.1 it is shown how the rod-on-disc results may be used to predict the temperature rise for a complete gear. This avoids the problem of redesign of a complete gear and/or gear train should excessive temperature rise become evident.

2.4. Steel rod axially aligned on disc

The polymer discs were made from Delrin 100 (Polyoxymethylene, POM). The experimental hardware (Fig. 3) consisted of a 100 W brushless DC electric motor driving a small 5:1 reduction epicyclic gearbox. The gearbox was connected, via a flexible coupling, to a steel shaft. The polymer disc was keyed to this shaft and so could be rotated up to a maximum speed of 800 rev/min. Motor

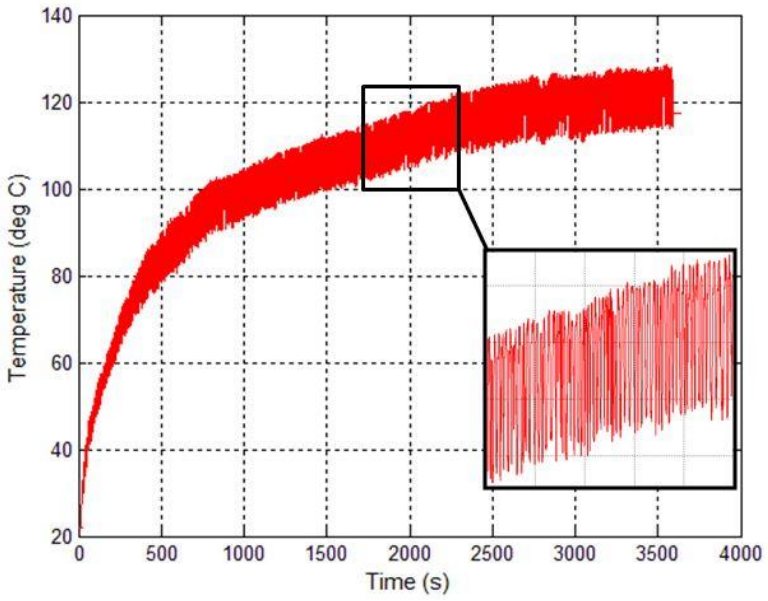

Fig. 5. Trial run of measured disc surface temperature to determine the required measurement time.

speed was measured by way of a Hall Effect surface mount encoder sensing the angular position of a small magnet attached to the rear of the motor shaft. The steel rod was held by an aluminium block, which was bolted to the load transducer. This consisted of a mild steel bar that had been machined to amplify the strain at a specific point. A full bridge strain gauge was adhered to the steel bar in the position of the maximum strain. The surface temperature of the disc was measured using an infrared sensor, the positioning of which in relation to the disc surface is shown as an inlay to Fig. 3. It was approximately 5 mm from the disc and was adjusted for an emissivity value of 0.91 for the device calibration, as provided by Beardmore [26].

The speed of rotation of the disc and the load applied through the rod were both calibrated using external measurements and were found to be within a 0.5% tolerance band. An investigation was made as to the magnitude of any fluctuations that may be present in the temperature data resulting from manufacturing tolerances. Figure 4 (a) shows the temperature of the disc surface, measured with maximum time resolution. Starting from a thermally heated state, the temperature decays for around 8 s at which point the disc was rotated at approximately 1 Hz. The fluctuation of the surface temperature can be seen clearly as the bulk of the material continues to cool, which is attributable to load variations between the aligned rod and disc caused by slight out of concentricity of the disc (Fig. 4 (b)). The ±1 deg C variations were considered to be within bounds for follow-on experimental investigations.

The aim was to measure surface temperature rise in the disc at a variety of speeds that would correspond with a series of positions along the line of contact in a real gear pair. Figure 5 shows a trial run of the experiment at full speed and load for 1 hour. The detailed view between 30–40 minutes shows the temperature fluctuations caused by the varying load. The temperature rise in the disc is

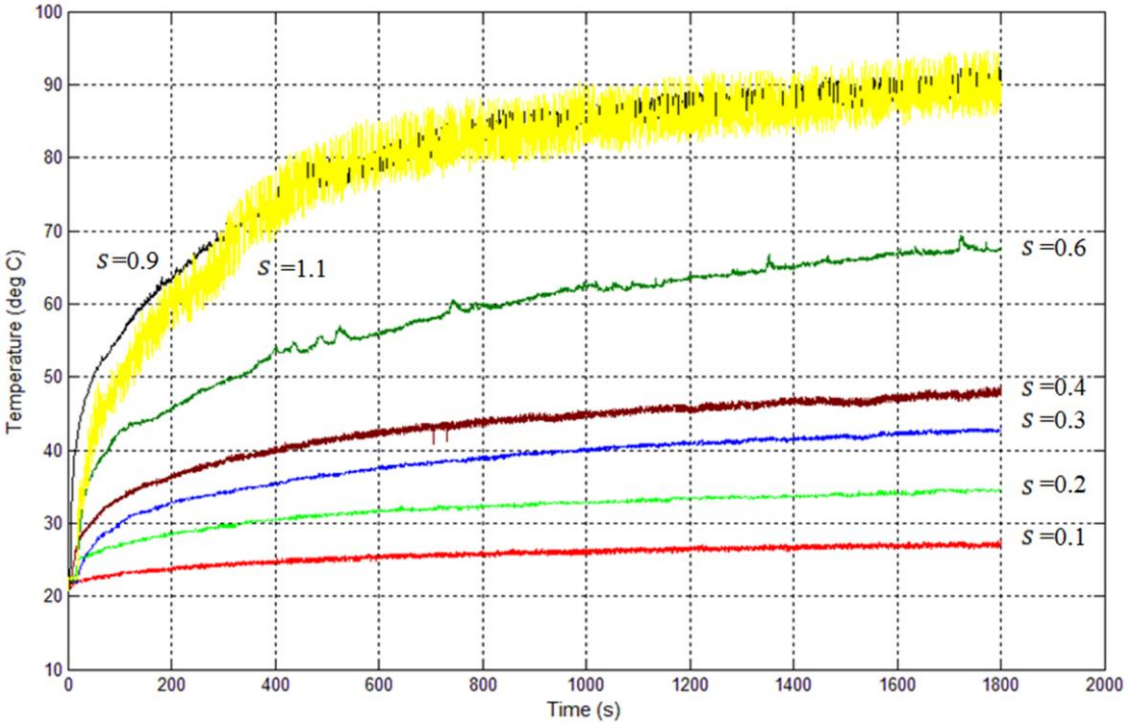

Fig. 6. Aligned rod on disc temperature results.

initially steep, but the rate of temperature rise decreases with time. An overall bulk increase of temperature of the experimental hardware (aluminium housing, plate, motor and gearbox) also gave rise to an additional increase in surface temperature. There are two distinct knee points of the data at 700 s and 2,800 s. These represent conditions of saturated bulk heating and a limit to the experimental time was therefore set at 1,800 s.

In association with Table 1, the corresponding disc rotational speeds, ω, are given in Table 2. Figure 6 shows the measured temperature corresponding to slip speeds associated with s over the range 0.1 mm to 1.1 mm. Surface temperatures of the disc increase as the slip speed increases until it is seen that the data sets for 0.9 mm and 1.1 mm overlap. Also, the 1.1 mm set exhibits a higher level of temperature fluctuation as time increases, which is attributable to amplified load variations.

Table 2

Correspondence of speeds with gear contact position.

s (mm)	**0.0**	**0.1**	**0.2**	**0.3**	**0.4**	**0.6**	**0.9**	**1.1**	**1.4**
v (mm/s)	0	61	121	182	243	364	547	668	850
ω (rev/min)	0	45	91	138	184	275	414	505	643

Table 3

Pinion/Gear data.

	Pinion	Gear
N° of Teeth	12	75
Torque	0.85 Nm	5.3 Nm
Speed	168 rev/min	26.7 rev/min
Power	15 W	<15 W
Module	1	1
Pressure Angle	20°	20°
Reference Diameter	12 mm	75 mm
Material	Steel 1.0511	POM
Profile Shift	+0.5	-0.5
Method of Manufacture	Hobbed	Hobbed

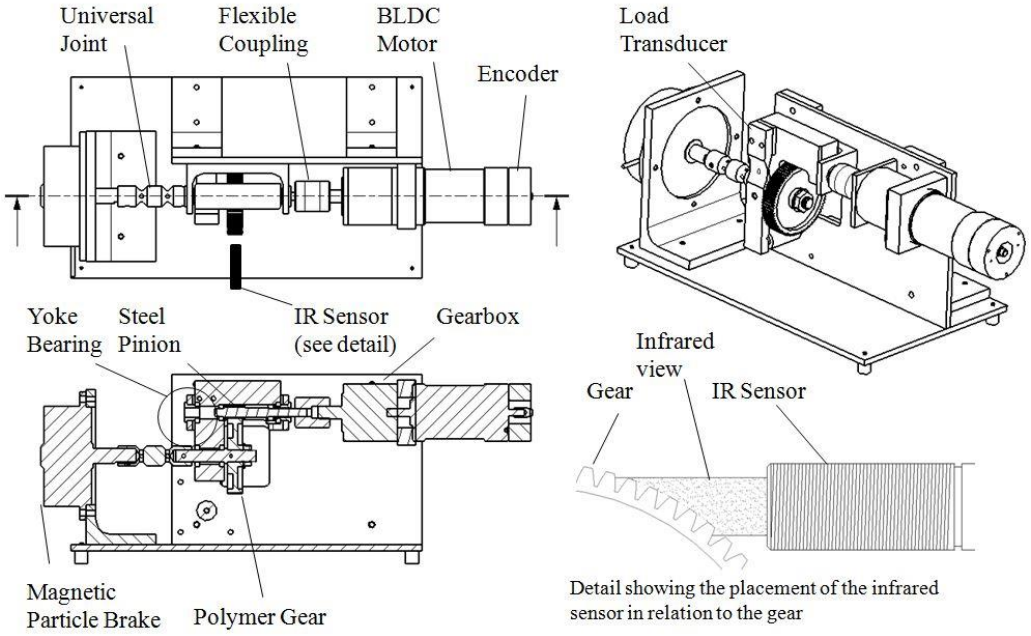

Fig 7. Gear running experimental hardware

2.5. Temperatures for a gear pair

This experiment used the same motor, load transducer assembly and control electronics as in the previous axially aligned rod on disc setup. This arrangement, however, drives a pair of gears together under a constant load and speed. Figure 7 shows the experimental hardware. Pertinent data are given in Table 3.

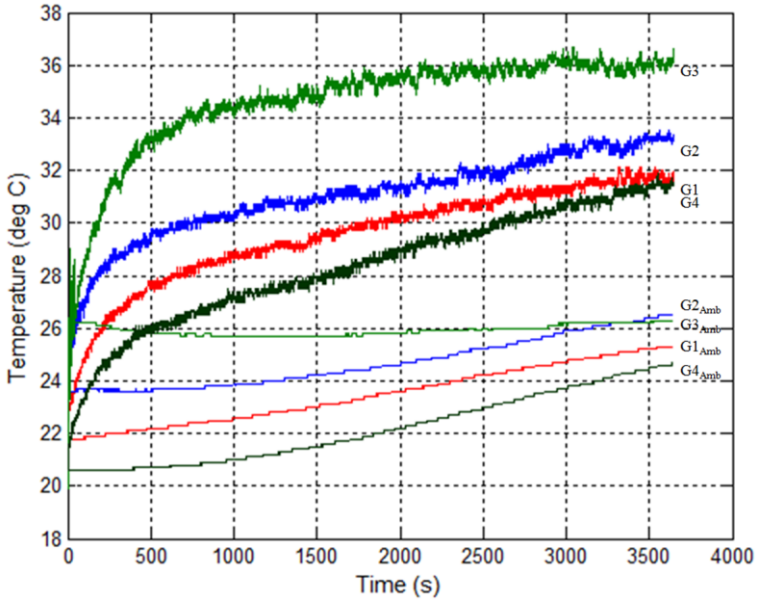

Fig. 8. Measured gear running temperatures.

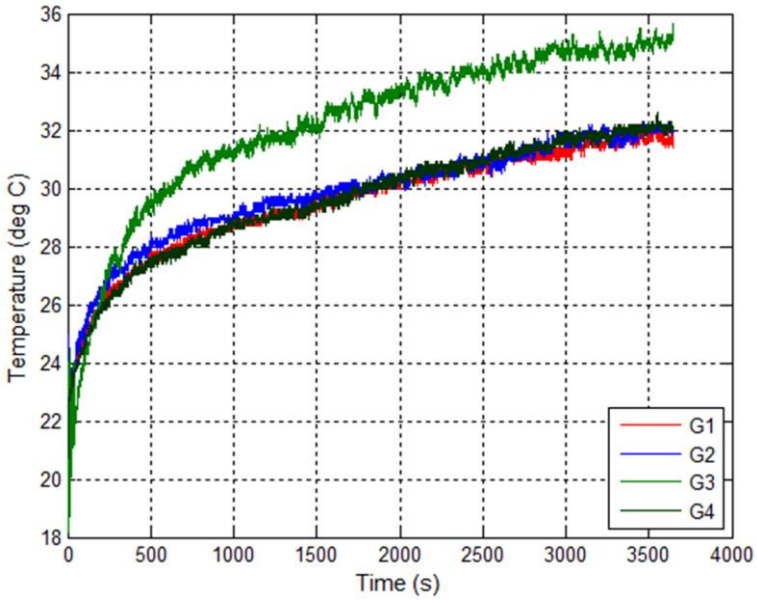

Fig. 9. Gear running temperatures - adjusted for ambient.

The motor drives the steel pinion, which is supported in two concentric bearings; the first allows the pinion to rotate and the second allows the frame in which the pinion is mounted to also rotate. This frame holds the polymer gear. The output shaft from the polymer gear is connected to a magnetic particle brake. When a voltage is applied to the brake it provides a resistive load to the rotation of the output from the gear, which in turn attempts to rotate the frame. The frame is reacted back to the support structure through the load transducer and so the torque generated by the output shaft from the gear is measured directly. Gear temperature was measured using the same infrared sensor as in Fig. 3. This was positioned facing the polymer teeth directly as they exited from the gear mesh. The system

torque and speed were set using a trial gear, which was then replaced with the experimental gear and the experiment was started. The speed and torque of the input pinion was 168 rev/min and 0.85 Nm, respectively. Each run lasted for 1 hour to ensure that the temperature rise due to teeth contact had been captured. Four runs were undertaken and labelled in order as: G1, followed by G2 after 2.5 hours, followed by G3 after 1 hour, followed by G4 after 1 week. Figure 8 shows the measured temperature profiles. The second profile, G2, is slightly higher by approximately 2 deg C than the first, G1, while G3 is higher by around 4 deg C. The final profile, G4, was taken after a delay of a week so that all latent heat in the system had dissipated and it lies below G1. The ambient temperature data sets were also recorded and are presented in Fig. 8. The gear temperature data were then adjusted to account for the ambient temperature during each of the experiment runs. The data were adjusted with respect to the first run G1 in the following manner:

$$\mathrm{G2_{Adj}} = \mathrm{G2} - (\mathrm{G2_{Amb}} - \mathrm{G1_{Amb}})$$
$$\mathrm{G3_{Adj}} = \mathrm{G3} - (\mathrm{G3_{Amb}} - \mathrm{G1_{Amb}})$$
$$\mathrm{G4_{Adj}} = \mathrm{G4} + (\mathrm{G1_{Amb}} - \mathrm{G4_{Amb}})$$

Figure 9 shows the adjusted data. Runs G1, G2 and G4 are nearly coincident. However, G3, which was run with only a 1 hour delay after G2, is approximately 4 deg C higher in temperature than the others.

4. Thermal modelling for the axially aligned rod on disc

4.1 Finite element (FE) model

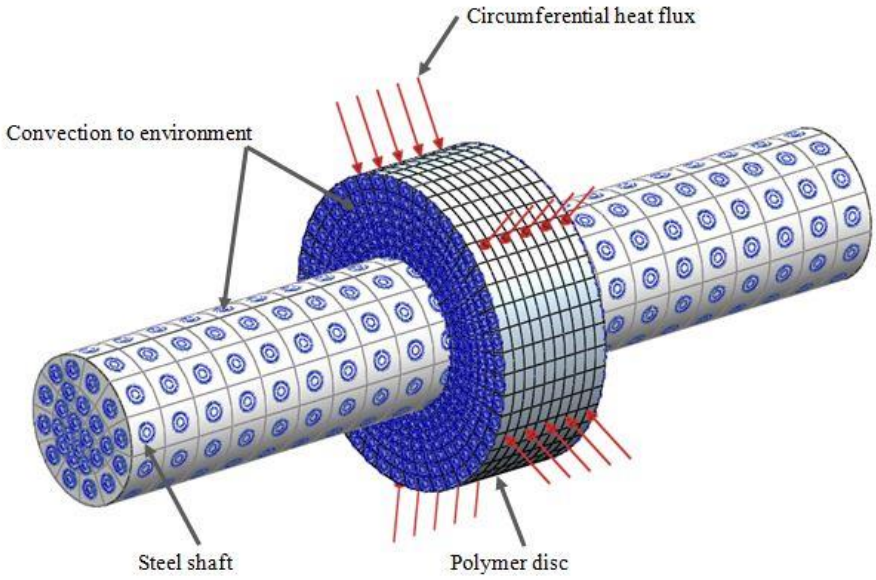

Fig. 10. Circumferential heat flux FE model.

Table 4

Model Parameters

	Disc	**Shaft**
Element type	20 Node Hexagonal	20 Node Hexagonal
Element number	3080	572
Element size	1 mm	3.4 mm
Element Material	POM	Steel

A solver was used and the following heat transfer coefficients were applied:

(a) 200 W/m^2/deg C between the shaft and the disc

(b) 12 W/m^2/deg C shaft to the environment

(c) 1.9 W/m^2/deg C the disc to environment

The heat load of 0.13 W was uniformly distributed on the outer circumferential surface of the polymer disc.

A FE model of the aligned rod and disc arrangement, without rotation, was established to provide an initial assessment of the thermal response. Figure 10 shows the meshed shaft and disc. The finite element model has been developed as a design environment alternative to the full analytical model described in Section 4.5. A series of these models should be used in conjunction with the time averaging technique described in Section 5.1.1to determine the heat rise in a gear. A heat flux distribution is applied to the outer diameter of the polymer disc and convection boundary conditions to the environment were set up on the flanks of the disc and also on the external surfaces of the steel shaft. Since the model was non-rotational, an averaged heat flux was applied over the circumferential surface of the polymer disc. Firstly, a heat flux from the aligned rod to the polymer disc was evaluated according to Eq. (9). This was then scaled to distribute it over the complete circumferential surface according to

$$Q_{FET} = Q_T \frac{A_i}{A_d} \tag{10}$$

where Q_{FET} is the heat flux value of the circumferential distribution applied in the FE model, Q_T is heat flux generated under the aligned rod (Eq. (9)), A_i is the area of indentation of the rod on disc, and A_d is the circumferential area of the modelled disc. The heat flux was applied in a step-like manner and a time dependent solution was obtained for a point on the centreline of the disc, as shown in Fig. 11. Although the general trend is similar to the experimental measurements of Fig. 9, a more accurate dynamic thermal analysis from the rod heat flux is appropriate.

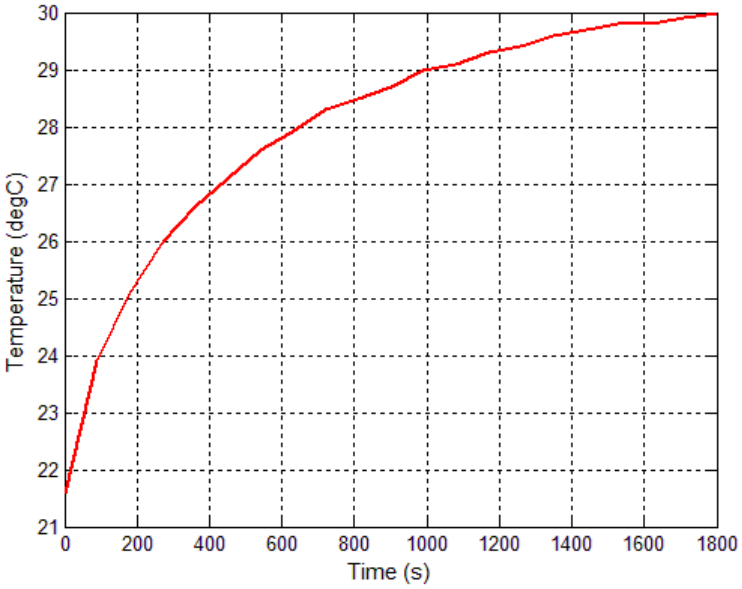

Fig. 11. Disc centreline surface temperature prediction from FE model.

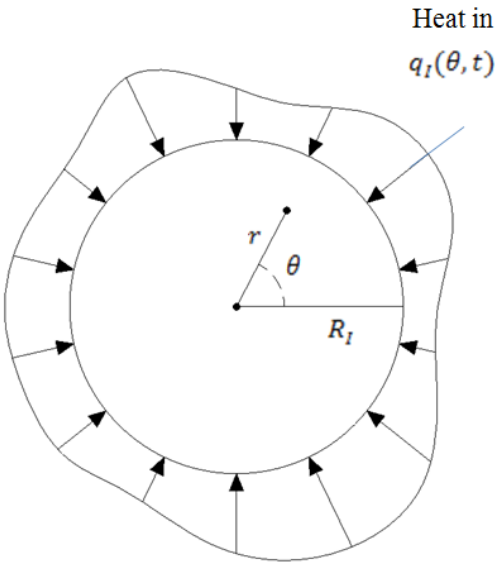

Fig. 12. Geometry and coordinates associated with the polymer disc analytical thermal model.

4.2 Analytical dynamic thermal model

Flash temperature predictions such as in Fig. 2 indicate behaviour in the immediate vicinity of contact between the two surfaces. However, cyclical thermal response due to rotation is not predicted. Higher order analytical modelling is possible, for example, to determine temperature rise generated in magnetic bearing touchdown events (Keogh and Yong [27]). Consideration is therefore given to the interaction of the steel rod in contact with the rotating polymer disc. The model is based around the heat transfer equation in polar coordinates (Fig. 12), which may be axially averaged across the width of the polymer disc:

$$\frac{\partial^2 T}{\partial r^2}+\frac{1}{r}\frac{\partial T}{\partial r}+\frac{1}{r^2}\frac{\partial^2 T}{\partial \theta^2}-\frac{1}{\alpha}\frac{\partial T}{\partial t}-\beta T=0 \tag{11}$$

where T is the axially averaged disc temperature relative to the ambient temperature, T_a, (r,θ) are polar coordinates, and

$$\alpha=\frac{k}{\rho c_p},\beta=\frac{2h}{Lk} \tag{12}$$

where k is the thermal conductivity of the polymer, ρ is its density, c_p is the specific heat capacity, L is the disc width, and h is a convection heat transfer coefficient. The boundary condition at the outer surface of a cylinder of radius $r=R_I$ is

$$k\frac{\partial T}{\partial r}\Big|_{r=R_I}=q_I(\theta,t) \tag{13}$$

where $q_I(\theta,t)$ is the axially averaged circumferential heat flux into the disc. Taking the Laplace transform of Eq. (11) yields

$$\frac{\partial^2 \overline{T}}{\partial r^2}+\frac{1}{r}\frac{\partial \overline{T}}{\partial r}+\frac{1}{r^2}\frac{\partial^2 \overline{T}}{\partial \theta^2}-\frac{p}{\alpha}\overline{T}-\beta\overline{T}=0 \tag{14}$$

where p is the Laplace transform variable. Expanding transformed temperature and heat flux as a Fourier series in the circumferential coordinate gives

$$\overline{T}(r,\theta,p)=\sum_{-\infty}^{\infty}\overline{T}_n(r,p)e^{in\theta},\overline{q}_I(\theta,p)=\sum_{-\infty}^{\infty}\overline{q}_{In}(p)e^{in\theta} \tag{15}$$

The equation of heat conduction becomes

$$\frac{\partial^2 \overline{T}_n}{\partial r^2}+\frac{1}{r}\frac{\partial \overline{T}_n}{\partial r}-\left(\frac{n^2}{r^2}+\frac{p}{\alpha}+\beta\right)\overline{T}_n=0 \tag{16}$$

The Bessel function solution that is finite as r tends to 0 is

$$\overline{T}_n(r,p)=A_n I_n(\lambda r) \tag{17}$$

where $\lambda=\sqrt{\frac{p}{\alpha}+\beta}$. The boundary condition of Eq. (13) is satisfied by

$$A_n=\frac{1}{k\lambda I_n'(\lambda R_I)}\overline{q}_{In}(p) \tag{18}$$

Hence

$$\overline{T}_n(r,p)=\frac{I_n(\lambda r)}{k\lambda I_n'(\lambda R_I)}\overline{q}_{In}(p) \tag{19}$$

The following recurrence relation (Abramowitz and Stegun [29]) applies:

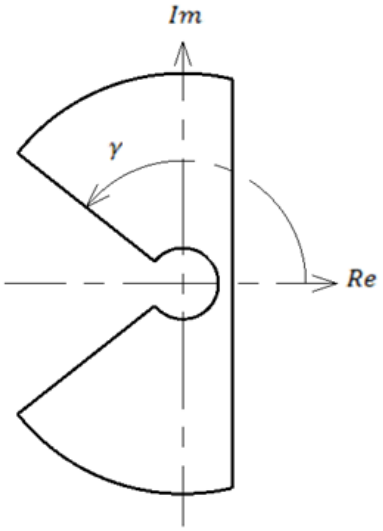

Fig. 13. Completion of the inversion contour.

$$I_n'(z) = I_{n+1}(z) + \frac{n}{z} I_n(z) \tag{20}$$

Equation (19) can then be inverted to give a solution in the time domain as

$$T_n(r,t) = \frac{1}{2\pi i} \int_{c-i\infty}^{c+i\infty} \frac{I_n(\lambda r)}{k\lambda \left(I_{n+1}(\lambda R_I) + \frac{n}{\lambda R_I} I_n(\lambda R_I) \right)} \overline{q}_{In}(p) e^{pt} dp \tag{21}$$

The temperature response may be obtained using the convolution integral

$$T_n(r,t) = \int_0^t H_n(r, t-\tau) q_{In}(\tau) dt \tag{22}$$

where

$$H_n(r,t) = \frac{1}{2\pi i} \int_{c-i\infty}^{c+i\infty} \frac{I_n(\lambda r)}{k\lambda \left(I_{n+1}(\lambda R_I) + \frac{n}{\lambda R_I} I_n(\lambda R_I) \right)} e^{pt} dp \tag{23}$$

Because $I_n\left(ve^{\pm\frac{1}{2}\pi i}\right) = e^{-\frac{1}{2}n\pi i} J_n(\mp v)$ has poles on the real axis it is appropriate to complete the contour of integration as shown in Fig. 13. In general, $p = z_\gamma \alpha x^2 / R_I^2$ on the angled lines where $x > 0$ and $z_\gamma = e^{i\gamma}$ on the upper line. Hence

$$dp = 2\frac{z_\gamma \alpha}{R_I^2} x dx, \quad \lambda_\gamma = \sqrt{\frac{z_\gamma x^2}{R_I^2} + \beta} \tag{24}$$

It now follows that

$$\frac{1}{2\pi i}\int_{c-i\infty}^{c+i\infty} f(\lambda)e^{pt}ds$$

$$= \frac{z_\gamma \alpha}{\pi i R_I^2}\int_0^\infty f(\lambda_\gamma)e^{\frac{z_\gamma \alpha x^2 t}{R_I^2}}xdx - \frac{z_{-\gamma}\alpha}{\pi i R_I^2}\int_0^\infty f(\lambda_{-\gamma})e^{\frac{z_{-\gamma}\alpha x^2 t}{R_I^2}}xdx \quad (25)$$

Since the second term is the complex conjugate of the first term, it follows that

$$\frac{1}{2\pi i}\int_{c-i\infty}^{c+i\infty} f(\lambda)e^{pt}dp = Re\left(\frac{2z_\gamma \alpha}{\pi i R_I^2}\int_0^\infty f(\lambda_\gamma)e^{\frac{z_\gamma \alpha x^2 t}{R_I^2}}xdx\right) \quad (26)$$

In this expression

$$z_\gamma f(\lambda_\gamma)x = \frac{2R_I^2}{Lk}h_n(x,\rho,\gamma)$$

$$h_n(x,\rho,\gamma) = \frac{z_\gamma x I_n\left(z_\gamma^{0.5}\rho x\right)}{\left(z_\gamma^{0.5}xI_{n+1}\left(z_\gamma^{0.5}x\right) + nI_n\left(z_\gamma^{0.5}x\right)\right)} \quad (27)$$

where $\rho = r/R_I$. It now follows from Eqs (22) and (23) that

$$T_n = H_n(r,t) = \frac{\alpha}{\pi i k R_I}\int_0^t\int_0^\infty \left\{h_n(x,\rho,\gamma)e^{\frac{z_\gamma \alpha x^2(t-\tau)}{R_I^2}} - h_n(x,\rho,-\gamma)e^{\frac{z_{-\gamma}\alpha x^2(t-\tau)}{R_I^2}}\right\}q_{In}(\tau)d$$

(28)

Considering the axially aligned rod and disc, the heat flux can be regarded as rotating at frequency ω about the circumference of the disc, which is considered to be stationary:

$$q_I(\theta,t) = Q_I(\theta - \omega t) \quad (29)$$

Hence

$$q_I(\theta,t) = \sum_{-\infty}^{\infty} Q_{In}e^{-in\omega t}e^{in\theta} \quad (30)$$

Then

$$q_{In}(\tau) = Q_{In}e^{-in\omega\tau} \quad (31)$$

Substituting into Eq. (28) and performing the time integration yields

$$T_n(r,t) = \frac{1}{2i}(T_{n,\gamma}(r,t) - T_{n,-\gamma}(r,t)) \quad (32)$$

where

$$T_{n,\gamma}(r,t) = \frac{2\alpha}{\pi k R_I}\int_0^\infty h_n(x,\rho,\gamma)\frac{e^{z_\gamma \alpha x^2 t/R_I^2}}{\left(z_\gamma \alpha x^2/R_I^2 + in\omega\right)}dxQ_{In} \quad (33)$$

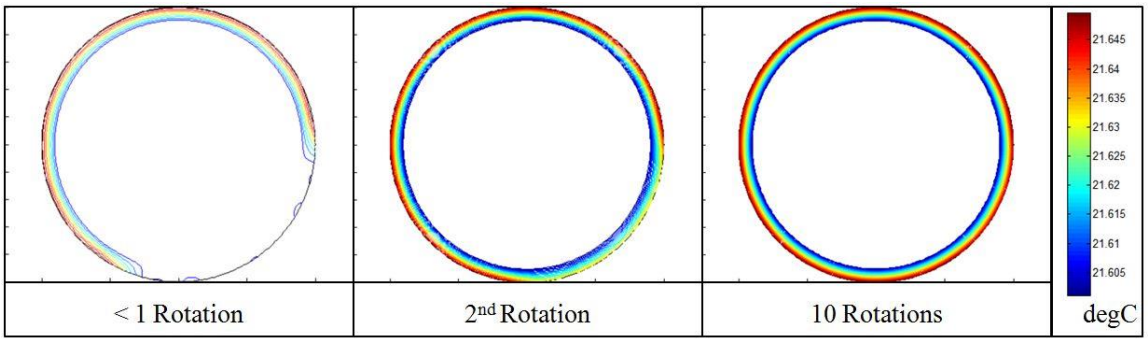

Fig. 14. Disc temperature contours for up to 10 rotations.

For a heat flux arising from a Hertzian pressure distribution between the aligned rod and disc, an appropriate expression for the heat flux into the polymer is

$$Q_I(\theta) = \begin{cases} Q_0\sqrt{(\theta_0^2 - \theta^2)}\ , & |\theta| < \theta_0 \\ 0\ , & |\theta| > \theta_0 \end{cases} \tag{34}$$

where $Q_0 = \phi\mu R_I\omega$ and $2\theta_0$ is the angular extent of the contact zone. The implication of Eq. (34) is that the Fourier coefficients follow as

$$Q_{In} = \begin{cases} \dfrac{Q_0\theta_0}{2n}J_1(n\theta_0)\ , & n \neq 0 \\ \dfrac{Q_0\theta_0^2}{2}\ , & n = 0 \end{cases} \tag{35}$$

The complete expression for the axially averaged disc temperature is

$$T(r,\theta,t) = \sum_{-\infty}^{\infty} T_n(r,t)e^{in\theta} \tag{36}$$

This expression was evaluated for the parameters matching the case when s = 0.2 mm. Time dependent contour plots of the disc temperature are shown in Fig. 14. The heat source moves in an anti-clockwise sense starting from the right hand side of the disc. After the second rotation it can be seen that the wall is starting to cool as the leading edge of the heat approaches the heat source for the third time. In the 10 rotation plot, the temperature is nearly uniform around the circumference of the disc.

Figure 15 shows the temperature variation at a fixed point on the circumference at 45° clockwise from the top of the disc. The initial step-like variation is due to the cyclic heating as the heat source (aligned rod) passes the observation point. The steps persist, though are not resolvable on the macro scale of the lower plot.

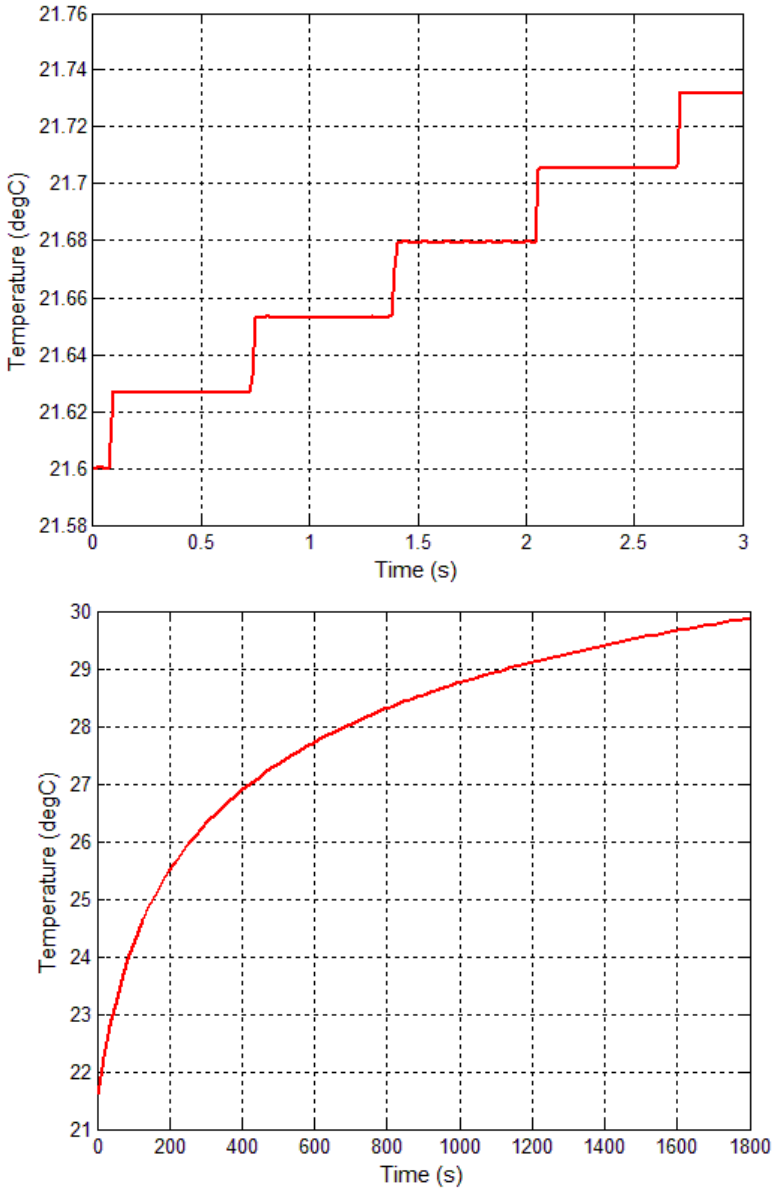

Fig. 15. Fixed point temperature variation with time.

5. Comparison and analysis of measured and modelled temperatures

The purpose of this section is to assess the level of correlation between the aligned rod on disc temperature measurements, the gear temperature measurements, and the predicted temperature measurements.

5.1 Aligned rod on disc and gear temperature measurement correlation

The temperature data for the aligned rod on disc need to be transformed so as to be useful to compare with the measured gear temperatures. The issue is that gear tooth slip speeds are variable during operation, while aligned rod on disc slip speeds are constant for each condition of test. The rod on disc measurements are therefore amalgamated to apportion results with appropriate to gear tooth

slip speeds at each point of the tooth sweep. The temperature generated at a given point in the tooth contact sweep is a function of both time and distance along the line of contact:

$$T_s = T(t, s) \tag{37}$$

where T_s is the temperature at the point along the line of contact s at time t. As the slip speed, v, varies through the contact sweep, the time increment spent in contact is given by

$$\delta t = \frac{1}{v}\delta s \tag{38}$$

Each aligned rod on disc temperature set ($i = 1, \dots, N$) is then averaged according to the time spent in contact to estimate the gear temperature as

$$T_{ave}(t) = \frac{1}{s_0}\sum_{i=1}^{N} T(t, s_i)\delta s_i \tag{39}$$

where s_0 is the length of travel along the line of contact. As the gear and pinion run together, heat flows into the polymer and the steel. As the teeth share contact, the heat generation will also be shared in the proportion given by the contact ratio, which is given by

$$R_C = \frac{\sqrt{\left({R_{go}}^2 - {R_{gb}}^2\right) + \left({R_{po}}^2 - {R_{pb}}^2\right)} - \sin\alpha}{d\cos\alpha} \tag{40}$$

where R_{go} is the outer radius of the gear, R_{gb} is the base radius of the gear, R_{po} is the outer radius of the pinion, R_{pb} is the base radius of the pinion, α is the pressure angle of the tooth form and d is the circular pitch of the teeth. Incorporating this factor of contact ratio into the summation of the data sets gives the correlated temperature as

$$T_{cor}(t) = \frac{R_C}{s_0}\sum_{i=1}^{N} T(t, s_i)\delta s_i \tag{41}$$

5.2 Comparison of gear temperatures with time averaged rod on disc temperatures and modelled temperatures

Figure 16 (a) shows the comparison of the summation of the averaged aligned rod on disc and gear temperature measurements. There is an offset between the two series of approximately 2.5 deg C. In Eq. (41), the contact ratio depends on the depth of the teeth and, in the case of the real product gear and pinion combination, a correction of 0.5 mm has been applied. This is to the addendum and dedendum of the gear teeth, which effectively moves the contact towards the gear centre. This is done to avoid undercutting and therefore weakening the teeth of the pinion during manufacture. The time averaging was repeated, including a 70 μm adjustment (reduction) to the contact radius. This was achieved by altering the values R_{go}, R_{gb}, R_{po} and R_{pb} in the contact ratio expression given in Eq.

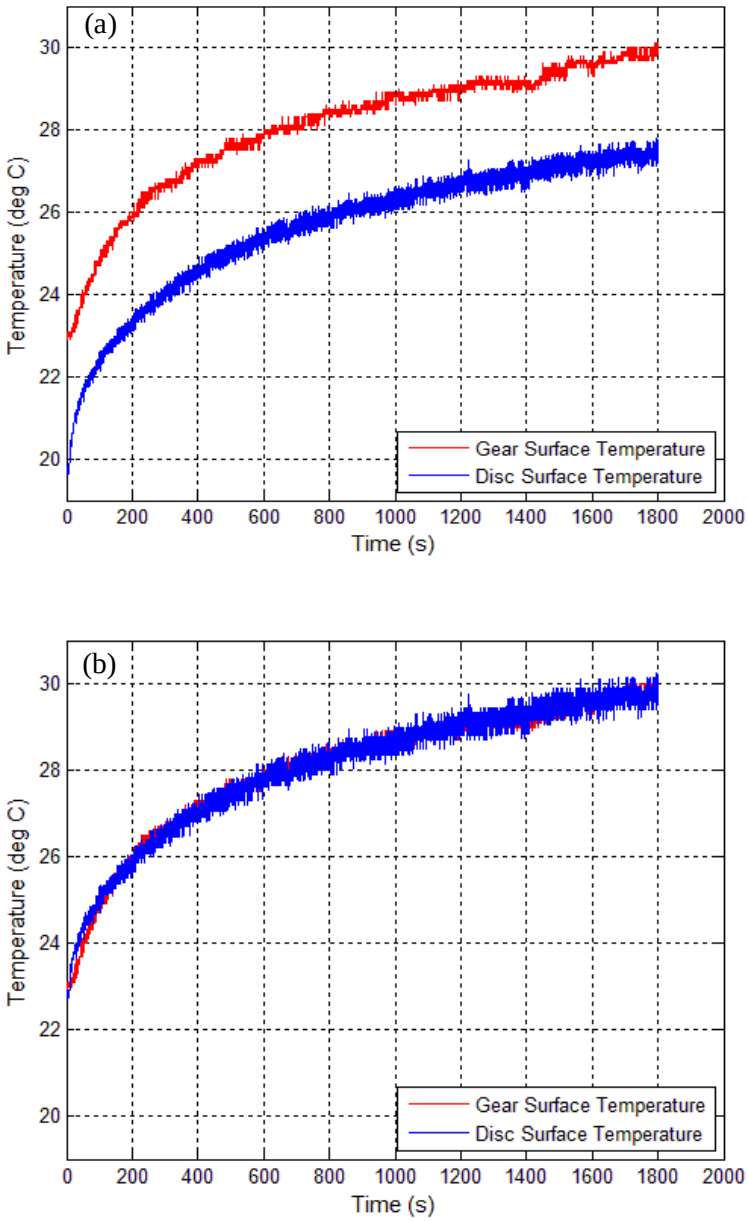

Fig. 16. Comparison of gear and disc temperature data.
(a) Without correction. (b) With 70 μm correction.

(40). The corrected averaged rod on disc temperature is shown in Fig. 16(b), which now aligns closely with the measured gear temperatures. It is therefore possible to use aligned rod on disc experimental data to evaluate the likely temperature rise in a real gear pair to within a tolerance determined by the accuracy of the manufactured gears.

Finally, the temperatures measured and time averaged from the rod on disc experiment can be compared to both the analytical and finite element models that have been presented. These data are also shown in Fig. 17 and good correlation exists between the three data sets. It is therefore possible to predict the running temperature of a polymer-steel spur gear pair using a simple aligned rod on disc

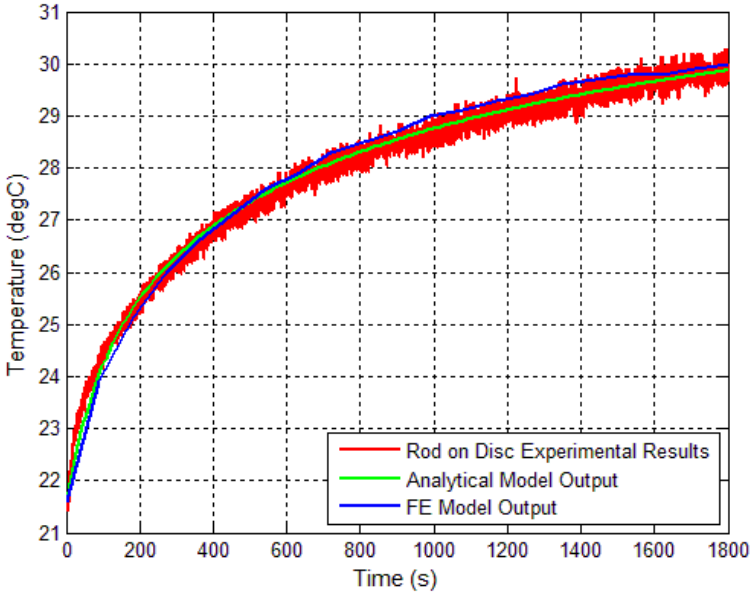

Fig. 17. Comparison of rod on disc temperatures with the model predictions.

model, either in analytical of finite element form. This is useful and convenient because, as previously discussed, a model that accurately represents the geometry and contact conditions of a spur gear pair would be excessively complex to construct and run.

6. Conclusions

An axially aligned steel rod on a polymer disc system is proposed for the prediction of the thermal response of a steel pinion and polymer gear, which is important for the assessment of gear efficiency. Losses arise from slip between the teeth. An experiment was therefore devised to measure thermal response of the polymer disc, with heating equivalent to local zones of contact between the gear teeth. The experiment was then augmented to enable the real gear pair to be run and the dynamic temperature of the polymer gear to be measured. The polymer disc and gear temperatures were then correlated through a novel technique of time averaging of the rod on disc results to integrate each temperature data set with respect to the gear contact sweep load profile. The initial correlation under-predicted the gear temperature results by around 9% or 2.5 deg C. This difference was attributed to manufacturing tolerance of geometric offsets, commonly introduced to prevent weakening of the pinion teeth during manufacture. A reduction of the reference radius from the gear centre 70 μm was considered appropriate and was shown to give rise to the under-prediction of 2.5 deg C.

Two models were also presented to predict the temperature rise in the aligned rod on disc experiment. The FE model considered an averaged circumferential heat input, whilst the analytical model included the rotational and cyclic nature of the heat input to the polymer disc. There was good

correlation between both models and the experimental data, which provides a degree of validation. It is therefore concluded that the combination of aligned rod on disc modelling and experimentation, together with time averaging over a gear contact load profile is sufficient to predict the running temperature of a spur gear pair. This avoids the need for complex transient analysis of the multiple interactions of teeth in a gear pair, which would be excessive if undertaken by FE modelling. Hence the methodology is appropriate for the design of new gear pairs in terms of the defined contact load profile.

References

[1] A.R. Breeds, S.N. Kukureka, K. Mao, D. Walton, C.J. Hooke, Wear behaviour of acetal gear pairs, Wear 166 (1993) 85–91.

[2] B.J. Hamrock, S.R. Schmid, B.O. Jacobson, Fundamentals of Fluid Film Lubrication (2nd edition, 2004), Marcel Dekker.

[3] C.J. Hooke, S.N. Kukureka, P. Liao, M. Rao, Y.K. Chen, The friction and wear of polymers in non-conformal contacts, Wear 200 (1996), 83–94.

[4] R.C. Bowers, W.C. Clinton, W.A. Zisman, Friction and lubrication of nylon, Industrial and Engineering Chemistry 46 (1954) 2416–2419.

[5] D. Walton, A.B. Cropper, D.J. Weale, P.K. Meuleman, The efficiency and friction of plastic cylindrical gears. Part 1: Influence of materials, Proceedings of the IMechE Part J: Journal of Engineering Tribology 216 (2002) 75–78.

[6] Y. Xie, J.A. Williams, The prediction of friction and wear when a soft surface slides against a harder rough surface, Wear 196 (1996) 21–34.

[7] J.A. Greenwood, J.B.P. Williamson, Contact of nominally flat surfaces, Proceedings of the Royal Society of London A: Mathematical, Physical and Engineering Sciences 295 (1966) 300–319.

[8] J. Fisher, D. Dowson, H.Hamdzah, H.L. Lee, The effect of sliding velocity on the friction and wear of UHMWPE for use in total artifical joints, Wear 175 (1994) 219–225.

[9] H. Blok, The flash temperature concept, Wear 6 (1963) 483–494.

[10] P. Samyn, G. Schoukens, Calculation and significance of the maximum polymer surface temperature T* in reciprocating cylinder-on-plate sliding, Polymer Engineering Science 48 (2008) 774–785.

[11] M. Conte, B. Pinedo, A. Igartua, Frictional heating calculation based on tailored experimental measurements, Tribology International 74 (2014) 1-6.

[12] K. Mao, A numerical method for polymer composite gear flash temperature prediction, Wear 262 (2007) 1321–1329.

[13] C.H. Kim, Durability improvement method for plastic spur gears, Tribology International 39 (2006), 1454–1461.

[14] H. Duzcukoglu, Study on development of polyamide gears for improvement of load carrying capacity, Tribology International 42 (2009) 1146–1153.

[15] C.J. Hooke, K. Mao, D. Walton, A.R. Breeds, S.N. Kukureka, Measurement and prediction of the surface temperature in polymer gears and its relationship to gear wear, ASME Journal of Tribology 115 (1992) 119–124.

[16] S. Senthilvelan, R. Gnanamoorthy, Efficiency of injection moulded polymer composite spur gears, Proceedings of the IMechE Part J: Journal of Tribology 223 (2009) 925–928.

[17] K. Mao, W. Li, C.J. Hooke, D. Walton, Friction and wear behaviour of acetal and nylon gears, Wear 267 (2009) 639–645.

[18] K. Mao, W. Li, C.J. Hooke, D. Walton, Polymer gear surface thermal wear and its performance prediction, Tribology International 43 (2010) 433–439.

[19] B. Vick, M.J. Furey, A basic theoretical study of the temperature rise in sliding contact with multiple contacts, Tribology International 34 (2001) 823–829.

[20] J.F. Archard, The temperature of rubbing surfaces, Wear 2 (1959) 438–455.

[21] D. Walton, A.A. Tessema, C.J. Hooke, J.M. Shippen, Load sharing in metallic and non-metallic gears, Proceedings of the IMechE, Part C: Journal of Mechanical Engineering Science 208 (1994) 81–87.

[22] M. Taburdagitan, M. Akkok, Determination of surface temperature rise with thermo-elastic analysis of spur gears, Wear 261 (2006) 656–665.

[23] H. Unal, U. Sen, A. Mimaroglu, Dry sliding wear characterisitics of some industrial polymers against steel counterface, Tribology International 37 (2004) 727–732.

[24] W.C. Young, R.G. Budynas, Roark's formulas for stress and strain (8th edition, 2011), McGraw-Hill.

[25] Y. Lee, Y. Liu, J.R. Barber, Y.H. Jang, Thermal considerations during transient asperity contact, Tribology International 94 (2016) 87-91.

[26] R. Beardmore, RoyMech [Online] Available at: http://roymech.co.uk/ [Accessed 28 February 2014].

[27] P.S. Keogh, W.Y. Yong, Thermal assessment of dynamic rotor/auxiliary bearing contact events, ASME Journal of Tribology 129 (2007) 143–152.

[28] M. Abramowitz, I.A. Stegun, Handbook of mathematical functions: with formulas, graphs, and mathematical tables (1967) US Government Printing Office.